

# Enhanced polyamine catabolism disturbs hematopoietic lineage commitment and leads to a myeloproliferative disease in mice overexpressing spermidine/spermine $N^1$ -acetyltransferase

Sini Pirnes-Karhu · Pentti Mäntymaa · Reijo Sironen · Petri I. Mäkinen ·  
Sara Wojciechowski · Sisko Juutinen · Jari Koistinaho · Sohvi Hörkkö ·  
Esa Jantunen · Leena Alhonen · Anne Uimari

Received: 30 April 2013 / Accepted: 25 June 2013 / Published online: 9 July 2013  
© Springer-Verlag Wien 2013

**Abstract** Spermidine/spermine  $N^1$ -acetyltransferase (SSAT) regulates intracellular polyamine levels by catabolizing spermidine and spermine which are essential for cell proliferation and differentiation. Hematological characterization of SSAT overexpressing mice (SSAT mice) revealed enhanced myelopoiesis and thrombocytopoiesis leading to increased amounts of myeloid cells in bone marrow, peripheral blood, and spleen compared to wild-type animals. The level of SSAT activity in the bone marrow cells was associated with the bone marrow cellularity and spleen weight which both were significantly increased in SSAT mice. The result of bone marrow transplantations indicated that both the intrinsic SSAT overexpression of bone marrow cells and bone marrow microenvironment had an impact on the observed hematopoietic phenotype. The Lineage-negative Sca-1<sup>+</sup>c-Kit<sup>+</sup> hematopoietic stem cell (HSC) compartment in SSAT

mice, showed enhanced proliferation, increased proportion of long-term HSCs and affected expression of transcription factors associated with lineage priming and myeloid differentiation. The proportions of common myeloid and megakaryocytic/erythroid progenitors were decreased and the proportion of granulocyte–macrophage progenitors was increased in SSAT bone marrow. The data suggest that SSAT overexpression and the concomitantly accelerated polyamine metabolism in hematopoietic cells and bone marrow microenvironment affect lineage commitment and lead to the development of a mouse myeloproliferative disease in SSAT mice.

**Keywords** Myeloproliferation · Hematopoiesis · Spermidine/spermine  $N^1$ -acetyltransferase · Polyamines

S. Pirnes-Karhu · P. I. Mäkinen · S. Wojciechowski ·  
S. Juutinen · J. Koistinaho · L. Alhonen · A. Uimari (✉)  
Biotechnology and Molecular Medicine, A.I. Virtanen Institute  
for Molecular Sciences, Biocenter Kuopio, University of Eastern  
Finland, P.O. Box 1627, 70211 Kuopio, Finland  
e-mail: anne.uimari@uef.fi

P. Mäntymaa  
Laboratory of Eastern Finland, Kuopio, Finland

R. Sironen  
Institute of Clinical Medicine, Pathology and Forensic Medicine,  
University of Eastern Finland, Kuopio, Finland

R. Sironen  
Department of Clinical Pathology, Kuopio University Hospital,  
Kuopio, Finland

R. Sironen  
Cancer Center of Eastern Finland, University of Eastern Finland,  
Kuopio, Finland

S. Hörkkö  
Department of Medical Microbiology and Immunology, Institute  
of Diagnostics, University of Oulu, Oulu, Finland

S. Hörkkö  
Clinical Research Center of Oulu University Hospital,  
Oulu, Finland

E. Jantunen  
Institute of Clinical Medicine, University of Eastern Finland,  
Kuopio, Finland

E. Jantunen  
Department of Medicine, Kuopio University Hospital,  
Kuopio, Finland

## Abbreviations

SSAT	Spermidine/spermine $N^1$ -acetyltransferase
ODC	Ornithine decarboxylase
AdoMetDC	s-adenosylmethionine decarboxylase
HSCs	Hematopoietic stem cells
AML	Acute myeloid leukemia
CML	Chronic myeloid leukemia
CMP	Common myeloid progenitors
MEP	Megakaryocyte-erythroid progenitors
GMP	Granulocyte/macrophage progenitors
LT-HSCs	Long-term hematopoietic stem cells
LSK cells	Lineage-negative Sca <sup>+</sup> c-Kit <sup>+</sup> cells

## Introduction

Polyamines are amino acid-derived polycationic molecules which affect cell proliferation and differentiation by regulating cell signaling, replication, transcription, and translation (Igarashi and Kashiwagi 2010). The diamine precursor of polyamines, putrescine, is synthesized from ornithine and further converted to higher polyamines, spermidine and spermine. Ornithine decarboxylase (ODC) and S-adenosylmethionine decarboxylase (AdoMetDC) are responsible for the rate-limiting biosynthetic steps of putrescine formation and production of the aminopropyl donor for the subsequent formation of spermidine and spermine, respectively. By way of a catabolic pathway, spermidine/spermine  $N^1$ -acetyltransferase (SSAT) is a key enzyme in the back conversion of spermine and spermidine to putrescine through acetylated forms of these polyamines. The polyamine metabolism is depicted in Fig. 1.

Since polyamines are essential for optimal cell growth, the depletion of cellular polyamines prevents cell proliferation. In contrast, the activity of the biosynthetic enzyme ODC and intracellular levels of polyamines are typically

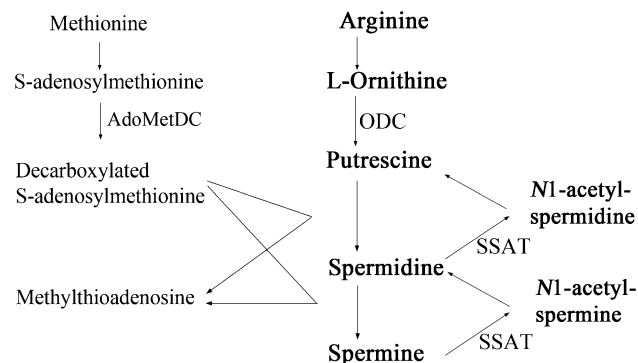


**Fig. 1** Polyamine pathway. Ornithine decarboxylase (ODC), S-adenosylmethionine decarboxylase (AdoMetDC) and spermidine/spermine  $N^1$ -acetyltransferase (SSAT)

increased in neoplastic cells (Thomas and Thomas 2003; Gerner and Meyskens 2004). The catabolic enzyme SSAT has a short half-life and is present at low quantities in resting cells. On the other hand, its amount and activity can be rapidly induced by multiple factors including polyamines, polyamine analogs, toxins, and stress pathways (Pegg 2008). Several studies using animal models and cultured cells have shown that induction of SSAT activity reduces tumor cell growth (Kee et al. 2004a, b; Vujcic et al. 2000; Jiang et al. 2007; Pledgie-Tracy et al. 2010). Contrary observations indicate that significantly higher SSAT activity is present in human breast cancer and colorectal cancer tissues than in the corresponding non-malignant tissues (Wallace et al. 2000; Linsalata et al. 2006). Although the enhanced SSAT activity in cancer can be considered as a secondary response to precancerous increase in ODC activity and polyamine pools to restore the growth control (Wallace et al. 2000) the overexpression of SSAT has also been associated with increased cancer susceptibility (Wang et al. 2007; Tucker et al. 2005).

Hematopoiesis initiates from hematopoietic stem cells (HSCs) and proceeds through committed progenitor cells to terminally differentiated blood cells. Leukemogenic events in HSCs and/or progenitor cells disturb blood cell production and differentiation leading to hematopoietic malignancies (Lane and Gilliland 2010). Bone marrow microenvironment also notably contributes to hematopoietic diseases (Askmyr et al. 2011). Polyamines and their analogs as well as the enzymes of polyamine metabolism have been indicated to have both therapeutic and prognostic value in leukemias. The AdoMetDC inhibitor methylglyoxal (bis) guanyldiurethane (MGBG) is effective against acute myeloid leukemia (AML) and chronic myeloid leukemia (CML), but the therapeutic use is limited by toxicity (Gastaut et al. 1987). ODC activity in peripheral blood mononuclear cells reflects the neoplastic proliferative activity in CML patients and has been suggested as an additional prognostic marker for CML (Tripathi et al. 2002). High spermine levels in erythrocytes of acute lymphoblastic leukemia (ALL) patients have been used to predict relapse (Bergeron et al. 1997). In addition, SSAT is differentially expressed during stages of CML which suggest its involvement in disease transformation and thus, influence of polyamine metabolism on the development of leukemias (Janssen et al. 2005).

To study the roles of polyamines in mammals, we have generated a mouse line overexpressing SSAT gene under its endogenous promoter (Pietila et al. 1997). Overexpression of SSAT leads to enhanced SSAT activity in the whole body and to concomitant depletion of spermidine and/or spermine as well as intracellular accumulation of putrescine and  $N^1$ -acetylspermidine (Alhonen et al. 2009). Here, we characterized the hematological phenotype of

SSAT mice. Our data indicate that SSAT overexpression in hematopoietic cells and bone marrow microenvironment disturbs hematopoietic lineage commitment and thus, hematopoietic homeostasis leading to a mouse myeloproliferative disease.

## Materials and methods

### Animals

Female and male transgenic mice overexpressing SSAT gene (Pietila et al. 1997) and their wild-type littermates in C57BL/6J background were used at the age indicated in each experiment. In bone marrow transplantations, the recipient mice were lethally irradiated twice with a dose of 5.5 Gy (fractions 3 h apart) 1 day before the transplantation. Donor bone marrow cells ( $5 \times 10^6$  cells/200  $\mu$ l of PBS-2 % FBS) were injected into the tail vein of the recipient mice under anesthesia. In cell proliferation studies, 1 mg of BrdU (BrdU Flow Kit, 557891, BD Biosciences, San Jose, CA, USA) in PBS was administered intraperitoneally 10–11 h before the sacrifice. All animal experiments were approved by the National Animal Experiment Board. Animals in housing facilities were regularly monitored for infectious pathogens, such as *Helicobacter* spp.

### Blood cell count

Peripheral blood was collected from hind leg saphenous vein into EDTA-coated tubes (BD Diagnostic, Franklin Lakes, NJ, USA). Automated blood cell count was performed by Sysmex k-4500 haematology analyser (Sysmex, Kobe, Japan).

### Isolation of mouse bone marrow cells

Bone marrow cells were flushed from the bone marrow cavity with PBS-10 % fetal bovine serum (FBS), and either filtered through 100- $\mu$ m nylon cell strainer (BD Diagnostic, Franklin Lakes, NJ, USA) for cell counting, flow cytometric analysis, and bone marrow transplantation or washed with PBS and subsequently used for determination of polyamine concentrations and enzyme activities.

### Flow cytometric analysis of spleen, peripheral blood, and bone marrow cells

Spleen tissue was crushed in PBS with 2 % FBS, filtered with 100- $\mu$ m nylon cell strainers (BD Diagnostic, Franklin Lakes, NJ, USA) then washed with PBS-2 % FBS solution. Red blood cells from spleen and blood single-cell

suspensions were lysed with red cell lysing buffer (BD Biosciences, San Jose, CA, USA) then washed with PBS-2 % FBS solution. Samples of  $1 \times 10^6$  cells in 50  $\mu$ l volume of PBS-2 % FBS solution were stained with antibodies and analyzed with FACSCalibur flow cytometer (BD Biosciences, San Jose, CA, USA) and analysed using CellQuest Pro software. Antibodies for CD3 (553067), CD4 (553653) and CD8 (553030) were purchased from BD Biosciences (San Jose, CA, USA) and antibodies for B220 (11-0452-82) and Treg (Mouse regulatory T cell staining kit #3) were purchased from eBioscience (San Diego, CA, USA). Analyses of bone marrow cells and sorting of LSK cells were performed on a FACSaria III flow cytometer using FACSDiva software (BD Biosciences, San Jose, CA, USA). The Mouse Hematopoietic Stem and Progenitor Cell Isolation Kit (560492), BrdU Flow Kit (557891), and CD117 antibody (553356) were purchased from BD Biosciences (San Jose, CA, USA). The CD16/CD32 antibody (12-0161), Mouse Hematopoietic Lineage Biotin panel (88-7774), and streptavidin (45-4317) were purchased from eBioscience (San Diego, CA, USA). The lineage positive cells were depleted by the mouse hematopoietic progenitor cell enrichment kit (19756, STEMCELL Technologies, Grenoble, France). All kits were used according to the manufacturers' instructions.

### Quantitative real-time PCR (qPCR) analysis

FACS-sorted LSK cells from six to eight mice were pooled and grown for 16 h at 37 °C in 5 % CO<sub>2</sub> in Iscove's modified Dulbecco's medium (IMDM) supplemented with 1 % BSA, 0.1 mM 2-mercaptoethanol, 2 mM glutamine, human transferrin (200  $\mu$ g/ml), bovine pancreatic insulin (10  $\mu$ g/ml), low density lipoproteins (40  $\mu$ g/ml), human Flt-3 ligand (100 ng/ml), human IL-11 (100 ng/ml), and murine SCF (50 ng/ml). Total RNA from LSK cells was isolated with the RNeasy Mini Kit (Qiagen, Valencia, CA, USA), DNase-treated with the DNA-free Kit (Ambion, Austin, TX, USA) and reverse transcribed into cDNA with the High Capacity cDNA Reverse Transcription Kit (Applied Biosystems, Carlsbad, CA, USA) according to the manufacturer's instructions. Quantitative PCR (qPCR) analysis of cDNA (3 ng in RNA-equivalents) was carried out in a total volume of 20  $\mu$ l using the StepOnePlus Real-Time PCR System and SYBR Green PCR Master Mix (Applied Biosystems, Foster City, CA, USA). Fold changes in gene expressions were calculated using the  $\Delta\Delta$ Ct method. Hypoxanthine-guanine-phosphoribosyltransferase gene (HPRT1) was used as a reference gene to normalize the data. Reactions were performed duplicates. The following primers were used: HPRT1 (NM\_013556.2) caggccagacttggtagt (forward), ttgcgctcatcttaggcttt (reverse); GATA1 (NM\_008089.1) actgggagcaacggctact (forward), tccgccagagtgtgtagt

(reverse); PU.1 (NM\_011355.1) tgcaaatggaagggttttc (forward), tgcggagaatcccagtagt (reverse); CEPBA (NM\_007678.3) gcagtgtgcacgtctatgct (forward), cccaaacatccctaaaccaa (reverse); GFI1 (NM\_010278.2) ggcaaaagattccaccagaa (forward), gcttgaagcctgtgtgcttt (reverse); GATA2 (NM\_008090.5) aacgcctgtggcctctacta (forward), tggagagctcctcgaaacat (reverse); BMI1 (NM\_007552.4) cctgtgtggagggtacttca (forward), tggctgtgtttgtgaacct (reverse); HOXB4 (NM\_010459.7) ctggatgcgcaaagtgtac (forward), gcgtcaggtagcgatttag (reverse).

#### Analysis of blood and bone marrow smears

Mouse peripheral blood or cellular content of bone marrow was spread on a microscope slide, air-dried and Giemsa-stained with REASTAIN Quick-Diff Kit (Reagents Ltd, Toivala, Finland). Analyses of smears were performed by an experienced laboratory hematologist (PM).

#### Measurement of serum total immunoglobulin levels

Total serum IgA, IgM, and IgG immunoglobulin levels were measured using chemiluminescent immunoassay as described earlier (Nissinen et al. 2011; Kankaanpää et al. 2009). White round bottom 96-well microtiter plates (Microfluor 2; Dynex Technologies, Chantilly, VA, USA) were coated with 2.5 µg/ml anti-mouse IgA, IgM, or IgG antibodies (Sigma-Aldrich, St. Louis, MO, USA) in PBS buffer containing 0.27 mmol/l EDTA (PBS-EDTA) overnight at 4 °C. The plates were blocked with 0.5 % (w/v) fish-gelatin PBS-EDTA buffer and the serum samples were diluted 1:500, 1:5,000 and 1:10,000 (IgA, IgM, and IgG, respectively). The amount of immunoglobulins captured from the plasma samples were detected using appropriate alkaline phosphatase conjugated secondary antibodies (Sigma-Aldrich, St. Louis, MO, USA), LumiPhos 530 substrate solution (Lumigen Inc., Southfield, MI, USA), and Victor3 multilabel reader (Wallac, Perkin Elmer Finland Oy, Turku, Finland). Purified mouse IgA, IgM, or IgG (Sigma-Aldrich, St. Louis, MO, USA) was used as a standard curve (0–200 ng/ml) on each plate.

#### Histology

After sacrifice with CO<sub>2</sub>, the spleen, lymph node, thymus, and liver samples were immediately immersed in 10 % formalin and fixed overnight. Femurs and tibiae were placed in 10 % formalin for 48 h, decalcified in 74-mM FeCl<sub>3</sub>/3 % HCl solution for 3–4 days, neutralized in 5 % sodium thiosulphate solution overnight and rinsed with water for 24 h. Tissue samples were embedded in paraffin, cut into 10-µm thick sections and stained with hematoxylin

and eosin. Histopathological analyses of the tissues were performed by an experienced histopathologist (RS).

#### Determination of polyamine concentrations and ODC and SSAT activities

Tissues and cells were homogenized in buffer containing 25-mM Tris/HCl (pH 7.4), 0.1-mM EDTA and 1-mM DTT. For cells, the buffer was supplemented with 0.1 % Triton-X and Complete protease inhibitor cocktail (05 892 953 001, Roche, Mannheim, Germany). The concentration of polyamines in the homogenates was measured with high-performance liquid chromatography (Hyvonen et al. 1992). ODC and SSAT activities in the supernatant fractions of centrifuged homogenates were performed as described previously by Janne and Williams-Ashman (1971) and Bernacki et al. (1995), respectively.

#### Statistical analysis

Data are presented as mean ± SD when applicable. GraphPad Prism 5.03 software package (GraphPad Software Inc., LaJolla, CA, USA) was used to perform the unpaired two-tailed Student's *t* test and Pearson's correlation analyses. *P* value <0.05 was considered to be statistically significant.

## Results

#### Hypercellularity in peripheral blood, bone marrow, and spleen of SSAT mice is dominated by myeloid cells

Automated blood cell counts from peripheral blood samples of SSAT mice and their wild-type littermates at different ages are presented in Table 1. There were significantly higher numbers of lymphocytes and neutrophils in SSAT mice than their wild-type littermates at 3 months. This led to an increased total leukocyte count. The number of neutrophils increased with time resulting in significantly elevated proportion of neutrophils. Analysis of blood smears confirmed the proportional increase of neutrophils in SSAT mice (data not shown). The number of platelets in SSAT mice was also significantly elevated from age of 2 months. Anemia was evident at 2 months then again at 7 months and older. Blast cells or proportional changes in the numbers of other white blood cells were not observed.

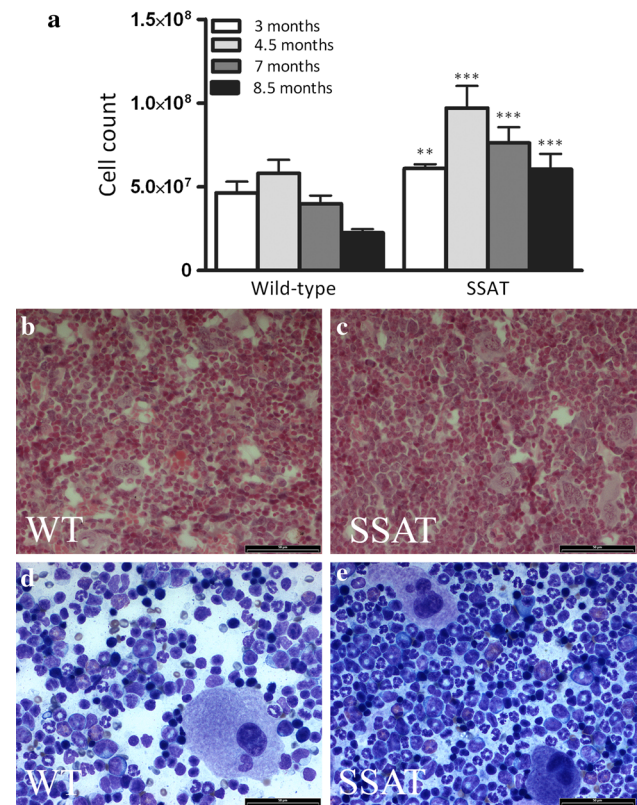
In bone marrow, the number of cells was significantly higher in SSAT mice than in their wild-type littermates (Fig. 2a). This hypercellularity was also evident histologically in hematoxylin and eosin-stained sections (Fig. 2b,

**Table 1** Blood count analyses of SSAT overexpressing (SSAT) and wild-type (wt) female mice at different ages

Age	Genotype	Leukocytes ( $\times 10^9/l$ )	Lymphocytes ( $\times 10^9/l$ )	Neutrophils ( $\times 10^9/l$ )	Lymphocytes (% of leukocytes)	Neutrophils (% of leukocytes)	Erythrocytes ( $\times 10^{12}/l$ )	Hemoglobin (g/l)	Platelets ( $\times 10^9/l$ )
2.5 weeks	Wt	5.4 $\pm$ 2.1	4.3 $\pm$ 1.6	1.0 $\pm$ 0.6	81 $\pm$ 9	17 $\pm$ 6	5 $\pm$ 1.5	77 $\pm$ 37	NM
	SSAT	5.5 $\pm$ 2.1	4.3 $\pm$ 1.4	1.1 $\pm$ 0.7	81 $\pm$ 6	19 $\pm$ 6	5.5 $\pm$ 0.5	79 $\pm$ 14	NM
1.5–2 months	Wt	16.2 $\pm$ 1.7	13.3 $\pm$ 1.7	2.7 $\pm$ 1.0	82 $\pm$ 4	18 $\pm$ 4	9.1 $\pm$ 0.2	152 $\pm$ 2	810 $\pm$ 220
	SSAT	20.2 $\pm$ 4.8	16.3 $\pm$ 3.4	3.6 $\pm$ 1.1	82 $\pm$ 2	18 $\pm$ 2	8.6 $\pm$ 0.5*	135 $\pm$ 7***	1200 $\pm$ 110*
4.5–5.5 months	Wt	5.70 $\pm$ 2	4.7 $\pm$ 1.3	1.0 $\pm$ 0.8	84 $\pm$ 7	16 $\pm$ 7	9.8 $\pm$ 0.3	163 $\pm$ 6	1400 $\pm$ 230
	SSAT	17.3 $\pm$ 3.2***	13.2 $\pm$ 2.1***	4.1 $\pm$ 1.4***	77 $\pm$ 5**	23 $\pm$ 5**	9.9 $\pm$ 0.4	162 $\pm$ 10	1450 $\pm$ 200
7–7.5 months	Wt	13.6 $\pm$ 3.3	11.5 $\pm$ 2.8	2.1 $\pm$ 0.6	85 $\pm$ 3	15 $\pm$ 3	9.8 $\pm$ 0.7	158 $\pm$ 5	1070 $\pm$ 300
	SSAT	16.1 $\pm$ 4.8	9.3 $\pm$ 5.2	6.8 $\pm$ 2.9***	54 $\pm$ 24***	46 $\pm$ 24***	8.8 $\pm$ 0.9***	132 $\pm$ 17***	1440 $\pm$ 300**
9.5 months	Wt	13.3 $\pm$ 2.5	10.9 $\pm$ 2.3	2.4 $\pm$ 0.4	82 $\pm$ 2	18 $\pm$ 2	9.0 $\pm$ 0.3	139 $\pm$ 7	1190 $\pm$ 180
	SSAT	20.1 $\pm$ 6.4*	6.3 $\pm$ 5.5*	13.8 $\pm$ 10.2**	36 $\pm$ 32**	64 $\pm$ 32**	7.2 $\pm$ 0.7***	110 $\pm$ 11***	1550 $\pm$ 280*

Data are presented as mean  $\pm$  SD,  $n = 4-18/\text{group}$ 

NM not measured

\*  $p < 0.05$ ; \*\*  $p < 0.01$ ; \*\*\*  $p < 0.001$  compared with wild-type mice**Fig. 2** SSAT mice have hypercellular bone marrow. **a** Bone marrow cell count of female (3, 7, and 8.5 months) and male (4.5 months) mice. The cell counts were calculated from femurs and tibiae of both hind limbs. Data are presented as mean  $\pm$  SD ( $n = 4-20$  per group). \*\* $p < 0.01$ , \*\*\* $p < 0.001$  compared with wild-type mice. **b–c** Hematoxylin–eosin stained tissue samples revealed hypercellular bone marrow of SSAT mice, no fibrosis was detected. **d–e** Giemsa-stained bone marrow smears indicated enhanced myelopoiesis and thrombocytopoiesis in SSAT mice (SSAT) compared with the wild-type animals (wt). Original magnification of  $\times 400$ 

c). The bone marrow architecture was normal and no fibrosis was detected. The bone marrow smears revealed enhanced myelopoiesis and thrombocytopoiesis in SSAT mice (Fig. 2d, e). The proportion of blast cells in the bone marrow was unchanged. Spleens of SSAT mice were enlarged (Fig. 3a, b) and their sizes correlated with the spleen cell number ( $r = 0.46$ ,  $p < 0.05$ ). Flow cytometric analysis confirmed increased proportion of granulocytic cells in peripheral blood, bone marrow, and spleen of SSAT mice (Fig. 3c). The histological sections of spleen, thymus, and liver revealed no architectural differences between SSAT and wild-type mice, and no infiltration of leukocytes or extramedullary hematopoiesis was observed in the liver (Fig. 3d).

Lymphocytes from adult mice were analyzed by flow cytometry. In spleen, the proportion of CD3<sup>+</sup> cells (T cells) was decreased and the proportion of B220<sup>+</sup> cells (B cells) was increased in SSAT mice when compared



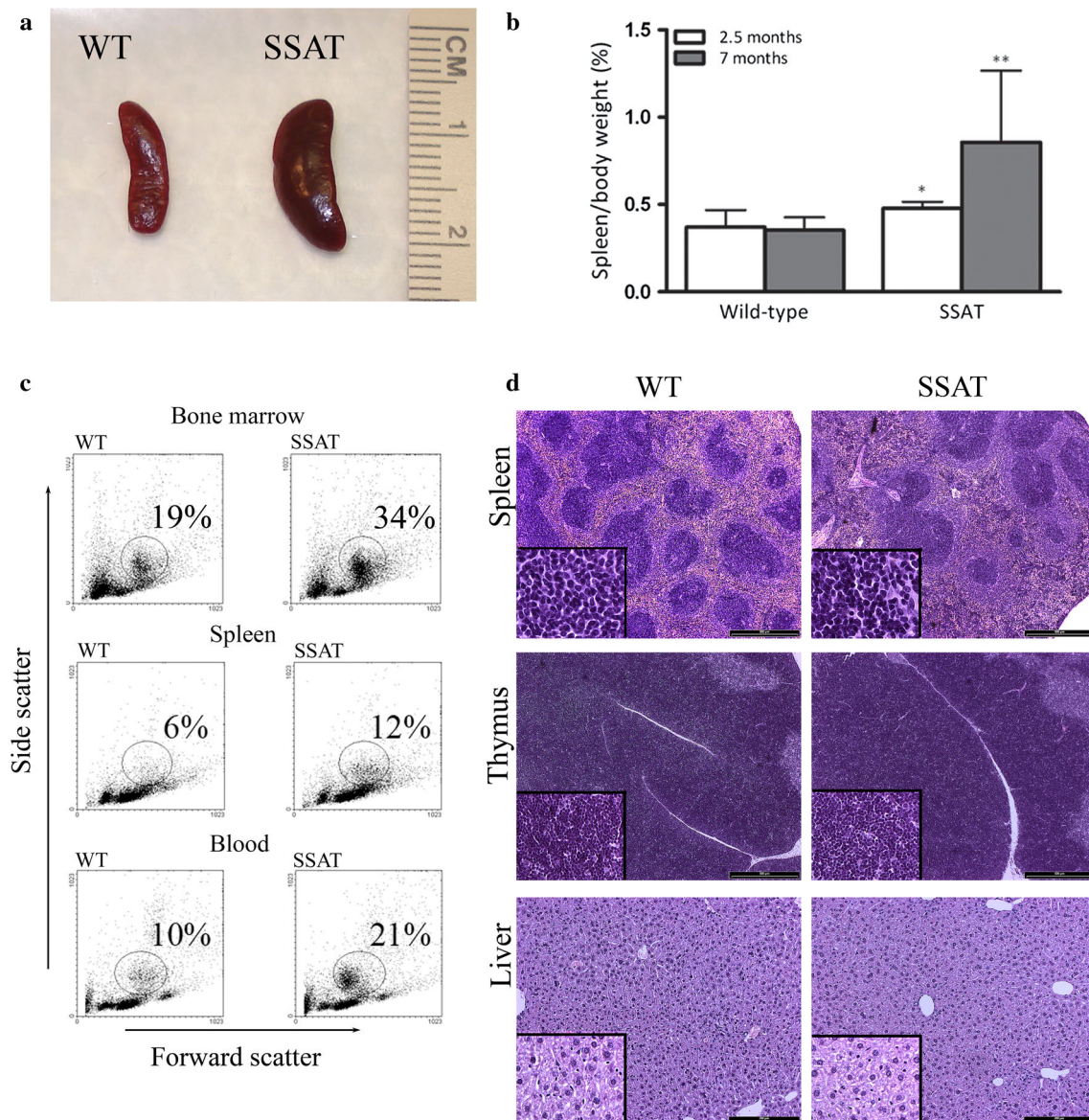


**Fig. 3** Immune tissues of SSAT mice accumulate myelogenous cells. **a** Enlarged spleen of SSAT mice. **b** Spleen weights of 2.5 and 7-month-old female SSAT mice (SSAT) and their wild-type littermates. **c** Flow cytometric analysis of granulocytic cells in bone marrow, spleen and peripheral blood of SSAT mice and their wild-type littermates (wt). Representative samples of 3-month-old female mice are shown. The numbers indicate the percentage of gated

granulocytic cells of total cell count. **d** The histological architecture of spleen, thymus and liver remained normal. Original magnification of  $\times 40$  and in *insets*  $\times 400$  (spleen),  $\times 40$  and in *insets*  $\times 200$  (thymus),  $\times 100$  and in *insets*  $\times 200$  (liver). Data are presented as mean  $\pm$  SD ( $n = 4$ – $20$  per group). \* $p < 0.05$ , \*\* $p < 0.01$  compared with wild-type mice

with the wild-type mice (Table 2). The ratio of CD4-positive helper T cells to CD8-positive cytotoxic T cells ( $CD4^+/CD8^+$ ) was significantly lower and the proportion of  $CD4^+CD25^+FoxP3^+$  cells (regulatory T cells) among  $CD3^+$  cells was significantly higher in the peripheral blood and spleen of SSAT mice. Serum from SSAT mice revealed IgA and IgM levels on par with wild-type, but revealed a marked increase of IgG (wt  $845 \pm 147 \mu\text{g/ml}$  serum, SSAT mice  $1160 \pm 246 \mu\text{g/ml}$  serum;  $p < 0.01$ ).

#### Cellularity of bone marrow and spleen correlates with bone marrow SSAT activity

Analysis of polyamine metabolism in SSAT bone marrow showed significantly increased SSAT and ODC activities which, respectively, led to a significantly decreased level of spermidine and an increased level of putrescine compared with the wild-type mice (Fig. 4a–c). Enhanced SSAT activity also led to the accumulation of  $N^1$ -acetylspermidine which was not detected in wild-type

**Table 2** Proportions of T (CD3<sup>+</sup>) and B (B220<sup>+</sup>) cells and helper (CD4<sup>+</sup>) and cytotoxic (CD8<sup>+</sup>) T cells in 4.5 months old male and regulatory T cells (CD4<sup>+</sup>CD25<sup>+</sup>FoxP3<sup>+</sup>) in 6.5 months old female SSAT overexpressing mice (SSAT) and their wild-type (wt) littermates

Tissue	Genotype	CD3 <sup>+</sup> cells (% of lymphocytes)	B220 <sup>+</sup> cells (% of lymphocytes)	CD3/B220 ratio	CD4 <sup>+</sup> cells (% of T cells)	CD8 <sup>+</sup> cells (% of T cells)	CD4/CD8 ratio	CD4 <sup>+</sup> CD25 <sup>+</sup> FoxP3 <sup>+</sup> cells (% of T cells)
Blood	Wt	31 ± 5	58 ± 8	0.5 ± 0.2	46 ± 5	26 ± 3	1.8 ± 0.2	1.7 ± 0.9
	SSAT	31 ± 6	62 ± 7	0.5 ± 0.2	39 ± 7	34 ± 4**	1.2 ± 0.3***	6.1 ± 0.7***
Spleen	Wt	43 ± 4	50 ± 5	0.9 ± 0.2	50 ± 10	21 ± 6	2.5 ± 0.7	11.5 ± 2.3
	SSAT	33 ± 1***	61 ± 3***	0.5 ± 0.04***	37 ± 6*	24 ± 4	1.6 ± 0.3*	16 ± 3.0*

Data are presented as mean ± SD, *n* = 6/group

\* *p* < 0.05; \*\* *p* < 0.01; \*\*\* *p* < 0.001 compared with wild-type mice

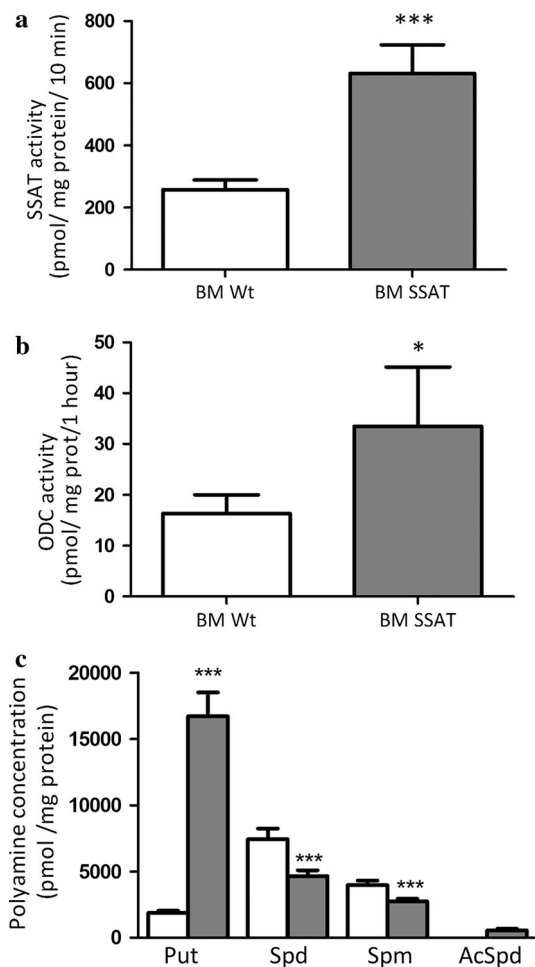


**Fig. 4** Polyamine metabolism in SSAT bone marrow is enhanced. **a** SSAT and **b** ODC activities and **c** polyamine amounts in wild-type (wt) and SSAT mice (SSAT) bone marrows. Putrescine (Put), spermidine (Spd), spermine (Spm), *N*<sup>1</sup>-acetylspermidine (AcSpd). Data are presented as mean ± SD (*n* = 5–12 per group, females and males). \**p* < 0.05, \*\*\**p* < 0.001 compared with wild-type mice

mice. Similar results were obtained from spleen, PBMC, and lymph nodes (data not shown). We noticed that SSAT activity and cellularity of bone marrow as well as

the weight of spleen varied among the transgenic individuals (see deviation in Figs. 2a, 3b, 4a). To analyze a possible relationship between the SSAT activity of bone marrow cells and cellularity of bone marrow and spleen, bone marrow SSAT activity was compared with the number of cells in bone marrow as well as with the size of the spleen in each mouse. The level of bone marrow SSAT activity correlated positively with the number of cells in bone marrow (*r* = 0.52, *p* < 0.05) and the weight of the spleen (*r* = 0.84, *p* < 0.001).

The myeloproliferative phenotype of SSAT mice is affected by both the intrinsic factors of bone marrow cells and bone marrow microenvironment

Lethally irradiated SSAT and wild-type mice received bone marrow cells from either SSAT or wild-type mice. Starting from 4 weeks post-transplantation, blood cell counts were taken every second week up to week 26 post transfer. Results of short-term transplantations (up to 10 weeks) indicated that the wild-type and SSAT recipients injected with SSAT bone marrow as well as the SSAT recipients receiving wild-type cells had increased proportion of peripheral blood neutrophils compared with the wild-type animals transplanted with wild-type bone marrow (Fig. 5). Long-term follow-up (up to 26 weeks) revealed that all SSAT recipients developed neutrophilia regardless of donor cells. The blood phenotype of wild-type mice that received SSAT cells attenuated to the level observed in the wild-type mice transplanted with the wild-type cells (Fig. 5). The bone marrow cells of SSAT recipients and the wild-type mice transplanted with SSAT bone marrow had increased SSAT activity, increased amount of putrescine as well as decreased levels of spermidine (data not shown). The number of bone marrow cells was increased only in the SSAT recipients (data not shown). However, the size of the spleen at the time of sacrifice (26 weeks) was significantly increased in all SSAT recipients as well as in the SSAT bone marrow transplanted

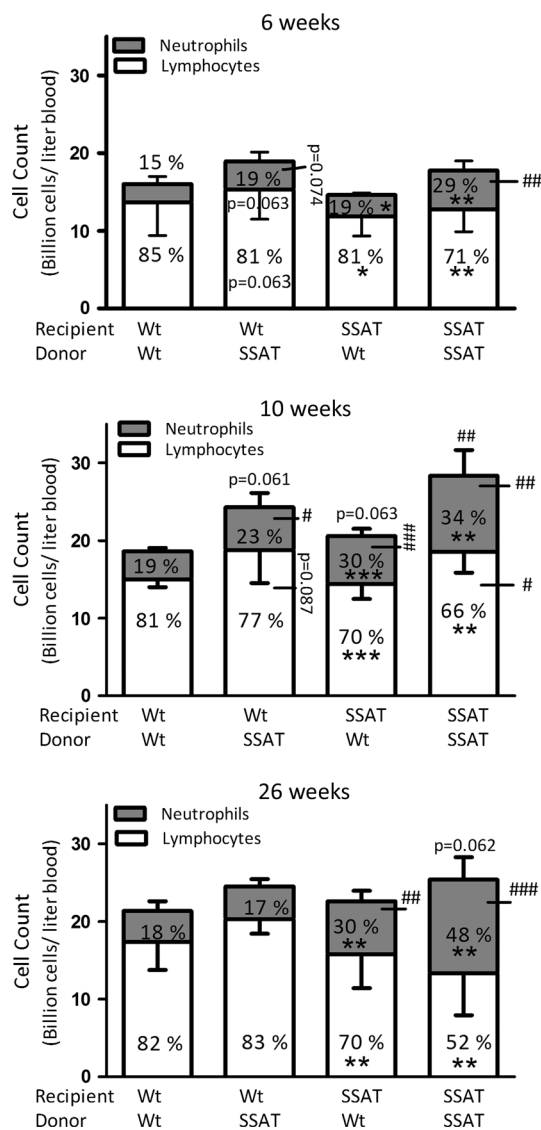


**Fig. 5** Intrinsic factors of bone marrow cells and bone marrow microenvironment influence the hematological phenotype of SSAT mice. Total white blood cell count and percentages of neutrophils and lymphocytes at 6, 10, and 26 weeks after transplantation. Wild-type (wt) and SSAT overexpressing (SSAT) recipient and donor mice are indicated. Data are presented as mean  $\pm$  SD ( $n = 8-10$  per group). \* $p < 0.05$ , \*\* $p < 0.01$ , \*\*\* $p < 0.001$  (percentages of neutrophils and lymphocytes); # $p < 0.05$ , ## $p < 0.01$ , ### $p < 0.001$  (total numbers of neutrophils and lymphocytes) compared with the values of wild-type recipients transplanted with the wild-type bone marrow

wild-type recipients compared with wild-type bone marrow transplanted wild-type mice (data not shown).

Altered gene expression in LSK cells of SSAT mice leads to changes in the bone marrow cell subpopulations

Flow cytometric analysis of the bone marrow cells showed changes in the cell numbers of all studied subpopulations in

SSAT mice compared with wild-type littermates (Fig. 6a). When the subpopulations were expressed as proportions of all bone marrow cells, a decrease in the amounts of common myeloid progenitors (CMP) and megakaryocyte-erythroid progenitors (MEP) were observed in SSAT mice (Fig. 6b, c). On the other hand, the proportions of granulocyte/macrophage progenitors (GMP) and long-term hematopoietic stem cells (LT-HSCs) were increased in 8-month-old SSAT mice (Fig. 6b, c). Proliferation of Lineage-negative Sca<sup>+</sup> c-Kit<sup>+</sup> cells (LSK, representing hematopoietic stem cells and multipotent progenitor cells), but not that of myeloid progenitors, was increased in SSAT mice compared with the wild-type mice (Fig. 6d). The distribution of LSK cells between the phases of cell cycle and the proportion of apoptotic LSK cells was similar in SSAT mice and wild-type mice (data not shown). Quantitative real-time PCR was performed to analyze the expression of myeloid lineage commitment regulators GATA-1, PU.1 and C/EBP $\alpha$ , as well as HSC self-renewal regulators Gfi1, Bmi1, GATA-2, and HoxB4. The LSK cells in SSAT mice showed enhanced GATA-1 and reduced PU.1 mRNA levels, whereas the expression of other studied transcription factors was comparable with wild-type mice (Fig. 6e).

## Discussion

In this study, we showed that the overexpression of SSAT in mice led to a disordered hematological phenotype dominated by myeloproliferation. The mice had an increased blood cell count along with increased numbers of non-lymphoid hematopoietic cells in spleen and bone marrow. Thus, they fulfilled the criteria of a myeloproliferative disease according to the Bethesda proposal for classification of murine non-lymphoid hematopoietic neoplasms (Kogan et al. 2002). Specifically, the myeloproliferative phenotype of SSAT mice included only mature cells in peripheral blood and spleen and showed no blast surplus in the bone marrow. In histological examination no changes affecting the typical spleen architecture with distinct red and white pulp were observed and thus, the enlargement of spleen was in all likelihood due to enhanced accumulation of peripheral blood white blood cells into the organ. After establishment at the age of 2 months, the myeloproliferative phenotype prevailed for the lifespan of the SSAT animals and was more pronounced in older mice. Proportional changes in splenic and/or peripheral B and T cell subpopulations as well as increase in serum IgG level in SSAT mice indicated that, at a minor extent, SSAT overexpression also affected lymphocytes. Our earlier immunological studies with SSAT mice supported also the notion that altered hematological phenotype of SSAT mice refers to a disorder. In the studies



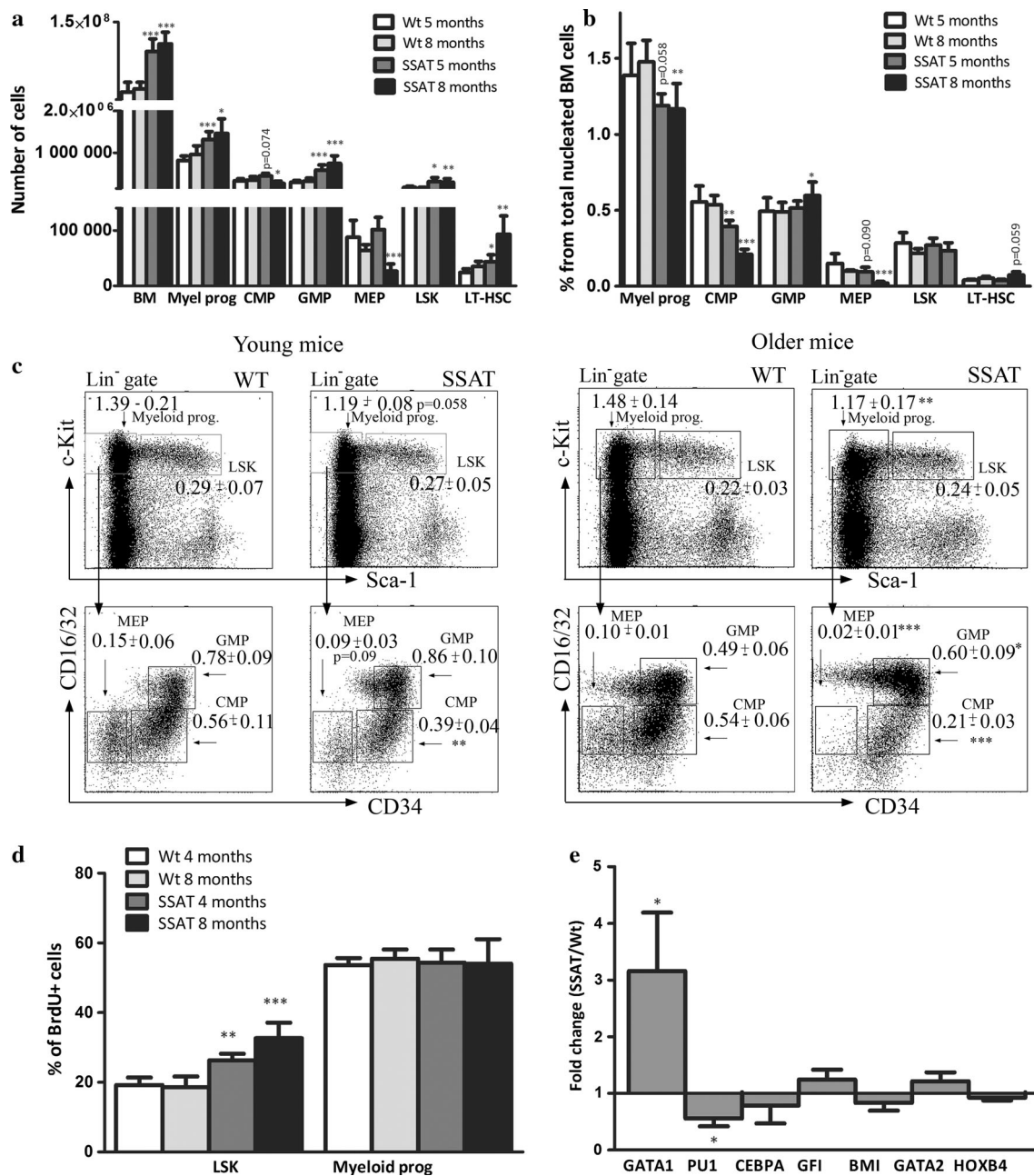


**Fig. 6** The numbers and functions of hematopoietic stem and progenitor cells are affected in SSAT mice. **a** Number and **b** percentages of cells in indicated populations within nucleated bone marrow (BM) cells obtained from tibiae and femurs of both hind limbs from young (5 months) and older (8 months) wild-type (WT) and SSAT mice ( $n = 6-8$  per group). **c** Representative profiles of flow cytometric stainings of lineage-negative bone marrow cells for c-Kit and Sca-1 (upper panels) and myeloid progenitors for CD16/32 and CD34 (lower panel) showing the percentages of given

populations within the total BM cells. **d** Percentage of BrdU-positive cells in indicated subpopulations in wild-type and SSAT mice ( $n = 6$  per group). **e** qPCR analysis showing fold changes in the expression levels of indicated transcription factors in sorted LSK cells of SSAT mice compared with the wild-type mice (value 1 represents the wild-type expression level). Samples in duplicates from three independent experiments were analyzed. \* $p < 0.05$ , \*\* $p < 0.01$ , \*\*\* $p < 0.001$  compared with the corresponding group of wild-type mice

of lipopolysaccharide (LPS)-induced endotoxic shock no changes in disease susceptibility, based on symptoms and mortality, to the toxin in SSAT mice compared with the wild-type animals were observed (Pirnes-Karhu et al.

2012). Interestingly, the molecular anti-inflammatory actions in the acute phase of LPS-induced immune response were enhanced in SSAT mice. In addition, the serum cytokine levels or the expression levels of acute phase

proteins in untreated SSAT mice were equal to untreated wild-type mice suggesting that SSAT mice did not suffer from chronic inflammation (Pines-Karhu et al. 2012).

The gene expression and flow cytometric analysis of SSAT mice bone marrow cells also supported the notion of disturbed hematopoiesis in these animals. In progenitor cells, the essential lineage commitment transcription factors GATA-1 and PU.1 primarily regulate erythromegakaryocytic and myelolymphoid differentiation, respectively (Laiosa et al. 2006). In HSCs, GATA-1 and PU.1 are expressed as part of the lineage priming process (Laiosa et al. 2006). PU.1 is also required for the maintenance of the HSC pool (Iwasaki et al. 2005). The LSK cells of SSAT mice showed significantly altered expression of GATA1 and PU.1 which most notably, influenced the characteristics of LSK cells and contributed to lineage commitment. The enhanced proliferation of LSK cells and diminished pools of CMPs and MEPs suggested accelerated differentiation of myeloid lineages. The view was also supported by the observations of enlarged GMP population and enhanced myelopoiesis in bone marrows of SSAT mice resulting in increased numbers of circulating peripheral blood and splenic neutrophils. Also the number of platelets was increased in SSAT mice, most probably at the expense of erythrocytes whose amount was decreased.

The hematopoietic microenvironment has been shown to be critical for the development of hematopoietic cells (Askmyr et al. 2011; Shen and Nilsson. 2012). It alone without intrinsic factors of hematopoietic cells can induce a hematological disorder as shown in mice with deficiency of retinoic acid receptor  $\gamma$  or Notch signaling resulting in myeloproliferation (Walkley et al. 2007; Kim et al. 2008). The bone marrow microenvironment is composed of multiple types of non-hematopoietic cells, including osteoblasts, mesenchymal stromal cells (MSCs), reticular stromal cells, endothelial cells, and nerve cells. They secrete factors which affect the HSC maintenance, but mostly, their exact roles in regulating hematopoiesis are unknown (Askmyr et al. 2011; Shen and Nilsson. 2012). The bone marrow transplantation experiments indicated that SSAT overexpressing bone marrow cells were able to transfer the myeloproliferative phenotype to the recipient mice irrespective of their genotype. Interestingly, wild-type bone marrow cells transplanted into SSAT recipients also resulted in SSAT mice-like blood count. The bone marrow cellularity and the proportion of neutrophils in the peripheral blood were enhanced by the SSAT genotype of recipient mice. The size of spleen remained enlarged also in the wild-type recipients of SSAT cells, but the long-term maintenance of the SSAT blood phenotype was only observed in SSAT mice recipients. Thus, the intrinsic factors of SSAT overexpressing bone marrow cells seemed to be able to induce the short-term myeloproliferation. Without the stimuli from SSAT bone

marrow microenvironment, this ability was weakened. Altogether, the transplantation experiments confirmed the important function of SSAT overexpressing bone marrow microenvironment in the development and maintenance of the disordered hematopoiesis in these animals. In addition, our recent findings of bone abnormalities and disturbed osteoblast function in SSAT mice further support the impact of non-hematopoietic cells on hematopoietic changes in these animals (manuscript in preparation). Characterization of SSAT mice will thus extend the current knowledge of interactions between bone, microenvironment, and hematopoiesis.

The severity of myeloproliferative phenotype was associated with the level of bone marrow SSAT activity. The main function of SSAT relates to catabolism of intracellular polyamines, spermidine and spermine which participate in multiple cellular processes. Recently, SSAT has been connected also with functions beyond regulation of polyamine homeostasis. SSAT has influence on the migration of  $\alpha 9 \beta 1$ -integrin expressing cells, like neutrophils and HSCs (Chen et al. 2004; deHart et al. 2008), and regulation of hypoxia-affected gene expression via degradation of hypoxia-inducible factor-1 (HIF-1) (Baek et al. 2007). It has been suggested that SSAT may also directly decrease cell proliferation by inactivating eukaryotic initiation factor 5A (eIF5A) through acetylation (Lee et al. 2010). Thus, both the disturbed polyamine homeostasis and the direct action(s) of SSAT could have affected the lineage commitment of hematopoietic cells and function of bone marrow microenvironment in SSAT mice. SSAT overexpression accelerates the polyamine flux by enhancing the action of metabolic enzymes and, thus, simultaneously increases the consumption of adenosine triphosphate (ATP) and acetyl coenzyme-A (acetyl-CoA), as well as production of  $H_2O_2$  and reactive aldehydes (Pirinen et al. 2007; Jell et al. 2007). In addition, mice overexpressing SSAT under the metallothionein promoter and having by many ways a similar phenotype as the SSAT mice have revealed signs of enhanced oxidative stress (Cerrada-Gimenez et al. 2011). The presence of oxidative stress has been observed in several myeloid malignancies, but its role in the pathogenesis of these diseases is unclear (Hole et al. 2011). However, it has been shown that high levels of reactive oxygen species increase the proliferation and reduce the self-renewal capacity of HSCs (Hole et al. 2011). Thus, the several metabolic consequences of enhanced SSAT expression may have contributed to myeloproliferation in SSAT mice and remain to be addressed in the future.

In summary, enhanced SSAT activity and/or consequently accelerated polyamine metabolism in hematopoietic cells and the bone marrow microenvironment of SSAT overexpressing mice are associated with disturbed lineage

commitment and lead to a mouse myeloproliferative disease. Thus, the SSAT mouse as a novel model of disturbed hematopoiesis can be used to define factors connected with the biology of hematopoietic cells as well as the development of hematopoietic malignancies.

**Acknowledgments** We gratefully acknowledge Ms Tuula Reponen, Ms Anne Karppinen, Ms Arja Korhonen, and Ms Marita Heikkinen for their skilful technical assistance. We thank the radiation therapy unit of Kuopio University Hospital for irradiation of the mice.

**Conflict of interest** The authors declare that they have no conflict of interest.

## References

- Alhonen L, Uimari A, Pietila M, Hyvonen MT, Pirinen E, Keinänen TA (2009) Transgenic animals modelling polyamine metabolism-related diseases. *Essays Biochem* 46:125–144
- Askmyr M, Quach J, Purton LE (2011) Effects of the bone marrow microenvironment on hematopoietic malignancy. *Bone* 48:115–120
- Baek JH, Liu YV, McDonald KR, Wesley JB, Zhang H, Semenza GL (2007) Spermidine/spermine N(1)-acetyltransferase-1 binds to hypoxia-inducible factor-1 $\alpha$  (HIF-1 $\alpha$ ) and RACK1 and promotes ubiquitination and degradation of HIF-1 $\alpha$ . *J Biol Chem* 282:33358–33366
- Bergeron C, Bansard JY, Le Moine P, Bouet F, Goasguen JE, Moulinoux JP, Le Gall E, Catros-Quemener V (1997) Erythrocyte spermine levels: a prognostic parameter in childhood common acute lymphoblastic leukemia. *Leukemia* 11:31–36
- Bernacki RJ, Oberman EJ, Seweryniak KE, Atwood A, Bergeron RJ, Porter CW (1995) Preclinical antitumor efficacy of the polyamine analogue N1, N11-diethylnorspermine administered by multiple injection or continuous infusion. *Clin Cancer Res* 1:847–857
- Cerrada-Gimenez M, Pietilä M, Loimas S, Pirinen E, Hyvönen MT, Keinänen TA, Jänne J, Alhonen L (2011) Continuous oxidative stress due to activation of polyamine catabolism accelerates aging and protects against hepatotoxic insults. *Transgenic Res* 20:387–396
- Chen C, Young BA, Coleman CS, Pegg AE, Sheppard D (2004) Spermidine/spermine N1-acetyltransferase specifically binds to the integrin  $\alpha$ 9 subunit cytoplasmic domain and enhances cell migration. *J Cell Biol* 167:161–170
- deHart GW, Jin T, McCloskey DE, Pegg AE, Sheppard D (2008) The  $\alpha$ 9 $\beta$ 1 integrin enhances cell migration by polyamine-mediated modulation of an inward-rectifier potassium channel. *Proc Natl Acad Sci USA* 105:7188–7193
- Gastaut JA, Tell G, Schechter PJ, Maraninchi D, Mascret B, Carcassonne Y (1987) Treatment of acute myeloid leukemia and blastic phase of chronic myeloid leukemia with combined eflornithine (alpha difluoromethylornithine) and methylglyoxal-bis-guanyl hydrazone (methyl-GAG). *Cancer Chemother Pharmacol* 20:344–348
- Gerner EW, Meyskens FL Jr (2004) Polyamines and cancer: old molecules, new understanding. *Nat Rev Cancer* 4:781–792
- Hole PS, Darley RL, Tonks A (2011) Do reactive oxygen species play a role in myeloid leukemias? *Blood* 117:5816–5826
- Hyvonen T, Keinänen TA, Khomutov AR, Khomutov RM, Eloranta TO (1992) Monitoring of the uptake and metabolism of aminoxy analogues of polyamines in cultured cells by high-performance liquid chromatography. *J Chromatogr* 574:17–21
- Igarashi K, Kashiwagi K (2010) Modulation of cellular function by polyamines. *Int J Biochem Cell Biol* 42:39–51
- Iwasaki H, Somoza C, Shigematsu H, Duprez EA, Iwasaki-Arai J, Mizuno S, Arinobu Y, Geary K, Zhang P, Dayaram T, Fenyus ML (2005) Distinctive and indispensable roles of PU.1 in maintenance of hematopoietic stem cells and their differentiation. *Blood* 106:1590–1600
- Janne J, Williams-Ashman HG (1971) On the purification of L-ornithine decarboxylase from rat prostate and effects of thiol compounds on the enzyme. *J Biol Chem* 246:1725–1732
- Janssen JJ, Klaver SM, Waisfisz Q, Pasterkamp G, de Kleijn DP, Schuurhuis GJ, Ossenkoppele GJ (2005) Identification of genes potentially involved in disease transformation of CML. *Leukemia* 19:998–1004
- Jell J, Merali S, Hensen ML, Mazurchuk R, Spornyak JA, Diegelman P, Kisiel ND, Barrero C, Deeb KK, Alhonen L, Patel MS, Porter CW (2007) Genetically altered expression of spermidine/spermine N1-acetyltransferase affects fat metabolism in mice via acetyl-CoA. *J Biol Chem* 282:8404–8413
- Jiang R, Choi W, Khan A, Hess K, Gerner EW, Casero RA Jr, Yung WK, Hamilton SR, Zhang W (2007) Activation of polyamine catabolism by N1, N11-diethylnorspermine leads to cell death in glioblastoma. *Int J Oncol* 31:431–440
- Kankaanpää J, Turunen SP, Moilanen V, Horkko S, Remes AM (2009) Cerebrospinal fluid antibodies to oxidized LDL are increased in Alzheimer's disease. *Neurobiol Dis* 33:467–472
- Kee K, Foster BA, Merali S, Kramer DL, Hensen ML, Diegelman P, Kisiel N, Vujcic S, Mazurchuk RV, Porter CW (2004a) Activated polyamine catabolism depletes acetyl-CoA pools and suppresses prostate tumor growth in TRAMP mice. *J Biol Chem* 279:40076–40083
- Kee K, Vujcic S, Merali S, Diegelman P, Kisiel N, Powell CT, Kramer DL, Porter CW (2004b) Metabolic and anti proliferative consequences of activated polyamine catabolism in LNCaP prostate carcinoma cells. *J Biol Chem* 279:27050–27058
- Kim YW, Koo BK, Jeong HW, Yoon MJ, Song R, Shin J, Jeong DC, Kim SH, Kong YY (2008) Defective notch activation in microenvironment leads to myeloproliferative disease. *Blood* 112:4628–4638
- Kogan SC, Ward JM, Anver, Berman JJ, Brayton C, Cardiff RD, Carter JS, de Coronado S, Downing JR, Fredrickson TN, Haines DC, Harris AW, Harris NL, Hiai H, Jaffe ES, MacLennan IC, Pandolfi PP, Pattengale PK, Perkins AS, Simpson RM, Tuttle, Wong JF, Morse HC 3rd, Hematopathology subcommittee of the Mouse Models of Human Cancers Consortium (2002) Bethesda proposals for classification of nonlymphoid hematopoietic neoplasms in mice. *Blood* 100:238–245
- Laiosa CV, Stadtfeld M, Graf T (2006) Determinants of lymphoid-myeloid lineage diversification. *Annu Rev Immunol* 24:705–738
- Lane SW, Gilliland DG (2010) Leukemia stem cells. *Semin Cancer Biol* 20:71–76
- Lee SB, Park JH, Folk JE, Deck JA, Pegg AE, Sokabe M, Fraser CS, Park MH (2010) Inactivation of eukaryotic initiation factor 5A (eIF5A) by specific acetylation of its hypusine residue by spermidine/spermine acetyltransferase 1 (SSAT1). *Biochem J* 433:205–213
- Linsalata M, Giannini R, Notarnicola M, Cavallini A (2006) Peroxisome proliferator-activated receptor gamma and spermidine/spermine N1-acetyltransferase gene expressions are significantly correlated in human colorectal cancer. *BMC Cancer* 6:191
- Nissinen AE, Laitinen LM, Kakko S, Helander A, Savolainen MJ, Horkko S (2011) Low plasma antibodies specific for phosphatidylethanol in alcohol abusers and patients with alcoholic pancreatitis. *Addict Biol* 17:1057–1067
- Pegg AE (2008) Spermidine/spermine-N(1)-acetyltransferase: a key metabolic regulator. *Am J Physiol Endocrinol Metab* 294:E995–E1010

- Pietila M, Alhonen L, Halmekyto M, Kanter P, Janne J, Porter CW (1997) Activation of polyamine catabolism profoundly alters tissue polyamine pools and affects hair growth and female fertility in transgenic mice overexpressing spermidine/spermine N1-acetyltransferase. *J Biol Chem* 272:18746–18751
- Pirinen E, Kuulasmaa T, Pietila M, Heikkinen S, Tusa M, Itkonen P, Boman S, Skommer J, Virkamaki A, Hohtola E, Kettunen M, Fatrai S, Kansanen E, Koota S, Niiranen K, Parkkinen J, Levonen AL, Yla-Herttuala S, Hiltunen JK, Alhonen L, Smith U, Janne J, Laakso M (2007) Enhanced polyamine catabolism alters homeostatic control of white adipose tissue mass, energy expenditure, and glucose metabolism. *Mol Cell Biol* 27:4953–4967
- Pirmes-Karhu S, Sironen R, Alhonen L, Uimari A (2012) Lipopolysaccharide-induced anti-inflammatory acute phase response is enhanced in spermidine/spermine N1-acetyltransferase (SSAT) overexpressing mice. *Amino Acids* 42:473–484
- Pledge-Tracy A, Billam M, Hacker A, Sobolewski MD, Woster PM, Zhang Z, Casero RA, Davidson NE (2010) The role of the polyamine catabolic enzymes SSAT and SMO in the synergistic effects of standard chemotherapeutic agents with a polyamine analogue in human breast cancer cell lines. *Cancer Chemother Pharmacol* 65:1067–1081
- Shen Y, Nilsson SK (2012) Bone, microenvironment and hematopoiesis. *Curr Opin Hematol* 19:250–255
- Thomas T, Thomas TJ (2003) Polyamine metabolism and cancer. *J Cell Mol Med* 7:113–126
- Tripathi AK, Chaturvedi R, Ahmad R, Asim M, Sawlani KK, Singh RL, Tekwani BL (2002) Peripheral blood leucocytes ornithine decarboxylase activity in chronic myeloid leukemia patients: prognostic and therapeutic implications. *Leuk Res* 26:349–354
- Tucker JM, Murphy JT, Kisiel N, Diegelman P, Barbour KW, Davis C, Medda M, Alhonen L, Janne J, Kramer DL, Porter CW, Berger FG (2005) Potent modulation of intestinal tumorigenesis in Apcmin/+ mice by the polyamine catabolic enzyme spermidine/spermine N1-acetyltransferase. *Cancer Res* 65:5390–5398
- Vujcic S, Halmekyto M, Diegelman P, Gan G, Kramer DL, Janne J, Porter CW (2000) Effects of conditional overexpression of spermidine/spermine N1-acetyltransferase on polyamine pool dynamics, cell growth, and sensitivity to polyamine analogs. *J Biol Chem* 275:38319–38328
- Walkley CR, Olsen GH, Dworkin S, Fabb SA, Swann J, McArthur GA, Westmoreland SV, Chambon P, Scadden DT, Purton LE (2007) A microenvironment-induced myeloproliferative syndrome caused by retinoic acid receptor gamma deficiency. *Cell* 129:1097–1110
- Wallace HM, Duthie J, Evans DM, Lamond S, Nicoll KM, Heys SD (2000) Alterations in polyamine catabolic enzymes in human breast cancer tissue. *Clin Cancer Res* 6:3657–3661
- Wang X, Feith DJ, Welsh P, Coleman CS, Lopez C, Woster PM, O'Brien TG, Pegg AE (2007) Studies of the mechanism by which increased spermidine/spermine N1-acetyltransferase activity increases susceptibility to skin carcinogenesis. *Carcinogenesis* 28:2404–2411